Journal of Biomechanics 42 (2009) 873–877

Contents lists available at ScienceDirect

Journal of Biomechanics

journal homepage: www.elsevier.com/locate/jbiomech
www.JBiomech.com

In situ mechanical properties of the chondrocyte cytoplasm and nucleus

Gidon Ofek [a,1], Roman M. Natoli [a,b,1], Kyriacos A. Athanasiou [a,*]

[a] Department of Bioengineering, Rice University, 6100 Main Street, Keck Hall Suite 116, Houston, TX 77005, USA
[b] MSTP, Baylor College of Medicine, One Baylor Plaza, N201, Houston, TX 77030, USA

ARTICLE INFO

Article history:
Accepted 21 January 2009

Keywords:
Unconfined cytocompression
Material properties
Mechanotransduction
Gene transcription

ABSTRACT

The way in which the nucleus experiences mechanical forces has important implications for understanding mechanotransduction. Knowledge of nuclear material properties and, specifically, their relationship to the properties of the bulk cell can help determine if the nucleus directly experiences mechanical loads, or if it is a signal transduction mechanism secondary to cell membrane deformation that leads to altered gene expression. Prior work measuring nuclear material properties using micropipette aspiration suggests that the nucleus is substantially stiffer than the bulk cell [Guilak, F., Tedrow, J.R., Burgkart, R., 2000. Viscoelastic properties of the cell nucleus. Biochem. Biophys. Res. Commun. 269, 781–786], whereas recent work with unconfined compression of single chondrocytes showed a nearly one-to-one correlation between cellular and nuclear strains [Leipzig, N.D., Athanasiou, K.A., 2008. Static compression of single chondrocytes catabolically modifies single-cell gene expression. Biophys. J. 94, 2412–2422]. In this study, a linearly elastic finite element model of the cell with a nuclear inclusion was used to simulate the unconfined compression data. Cytoplasmic and nuclear stiffnesses were varied from 1 to 7 kPa for several combinations of cytoplasmic and nuclear Poisson's ratios. It was found that the experimental data were best fit when the ratio of cytoplasmic to nuclear stiffness was 1.4, and both cytoplasm and nucleus were modeled as incompressible. The cytoplasmic to nuclear stiffness ratio is significantly lower than prior reports for isolated nuclei. These results suggest that the nucleus may behave mechanically different *in situ* than when isolated.

1. Introduction

How mechanical forces are experienced by the nucleus has important consequences for understanding mechanotransduction (Wang et al., 1993). Mechanotransduction is the process by which mechanical loads induce changes in the gene expression profile of a cell, which can ultimately alter cellular physiology and homeostasis. It has also been shown that alterations in the physical dimensions of the nucleus, resulting from an applied load on the tissue (Buschmann et al., 1996) or single cell (Leipzig and Athanasiou, 2008), correlate with changes in gene regulation. Previous investigation into the mechanical characteristics of isolated nuclei suggest that they behave like a viscoelastic material and are significantly stiffer than the cell as a whole (Guilak et al., 2000; Caille et al., 2002). However, these results are possibly influenced by the fact that the nuclei were removed from their *in situ* environment. The nuclear lamina, the framework for nuclear structure, is intimately linked to intermediate filaments positioned throughout the cytoplasm (Maniotis et al., 1997). Thus, mechanical properties of the nucleus may change when these connections are disrupted and the nucleus undergoes structural reorganization.

In this study, a finite element modeling approach was employed to obtain cytoplasmic and nuclear stiffness values which best match previously reported cellular and nuclear axial and lateral strains obtained during unconfined compression of single-attached chondrocytes (Leipzig and Athanasiou, 2008). Based on the nearly one-to-one correlation of cellular and nuclear strains observed in that study, we hypothesized the *in situ* nuclear stiffness is similar to that of the cytoplasm. Further, the effects of changing both cytoplasmic and nuclear Poisson's ratios were explored to investigate the validity of the commonly used assumption of cellular incompressibility.

2. Materials and methods

An axisymmetric model of the chondrocyte (height = 10 μm, width = 12 μm) with a nuclear inclusion (radius = 2.5 μm) was created using ABAQUS 6.7.1 (Fig. 1). The aforementioned geometric parameters were chosen to closely resemble an attached chondrocyte seeded for 3 h (Leipzig and Athanasiou, 2005; Koay et al., 2008). Both the nucleus and cytoplasm were modeled as isotropic linearly elastic solids. This elastic model was chosen, since the experimental data for cytoplasmic and nuclear strains were reported at equilibrium (Leipzig and Athanasiou, 2008), corresponding to long-time behavior of a viscoelastic solid (Leipzig and

* Corresponding author. Tel.: +1 713 348 6385; fax: +1 713 348 5877.
E-mail address: athanasiou@rice.edu (K.A. Athanasiou).
[1] These authors contributed equally to this work.

0021-9290/$ - see front matter © 2009 Elsevier Ltd. All rights reserved.
doi:10.1016/j.jbiomech.2009.01.024

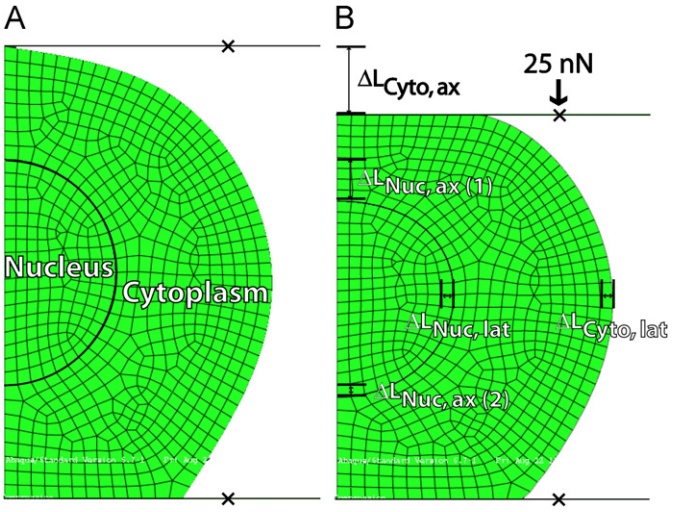

Fig. 1. Axisymmetric finite element depiction of a chondrocyte, with distinct nuclear and cytoplasmic regions, undergoing unconfined compression. In its undeformed state (A), the cell is considered to be 10 μm tall and 12 μm wide, with a spherical nuclear inclusion of radius 2.5 μm. The lateral and axial deformations of both the cytoplasm and nucleus were measured in response a 25 nN load applied onto the cell (B). The linear elastic mechanical properties of the cytoplasm and nucleus were varied parametrically, and a cost function (δ_{RMS}) value was calculated for each case in comparison to known experimental data (Leipzig and Athanasiou, 2008) (ax = axial; lat = lateral).

Athanasiou, 2005). Along the cell bottom, 4 μm of membrane was placed in frictionless contact with a rigid substrate. Preliminary analysis showed that substrate adhesiveness had no effect on the cytoplasmic and nuclear mechanical properties determined. Finally, the cell membrane was placed in frictionless contact with the compression platen. A reference point was created for the platen to which a 25 nN load was applied. The cytoplasm and nucleus consisted of 522 and 144 axially symmetric four node-reduced integration continuum elements (CAX4R), respectively. This was determined sufficient for convergence, as a model containing 2123 and 561 elements (cytoplasm and nucleus, respectively) yielded identical results.

To determine the combination of cytoplasmic and nuclear stiffnesses and Poisson's ratios that best-matched observed cytoplasmic and nuclear strains (Leipzig and Athanasiou, 2008), a root-mean-square difference cost function was used, defined as

$$\delta_{RMS} = \sqrt{(\varepsilon_{Axial}^{Model}(Nuc) - \varepsilon_{Axial}^{Experimental}(Nuc))^2 + (\varepsilon_{Axial}^{Model}(Cyto) - \varepsilon_{Axial}^{Experimental}(Cyto))^2 + (\varepsilon_{Lateral}^{Model}(Nuc) - \varepsilon_{Lateral}^{Experimental}(Nuc))^2 + (\varepsilon_{Lateral}^{Model}(Cyto) - \varepsilon_{Lateral}^{Experimental}(Cyto))^2}$$

δ_{RMS} was calculated for each combination of material properties. Lower δ_{RMS} values indicate that the model output more closely matched the previously reported data.

Briefly, as reported by Leipzig and Athanasiou (2008), cytoplasmic and nuclear strains were measured experimentally through the analysis of immunocytochemistry of cells fixed under a 25 nN compressive load. Cytomechanical testing was performed using a previously validated creep cytoindentation apparatus (Leipzig and Athanasiou, 2005; Leipzig et al., 2006; Shieh and Athanasiou, 2006; Eleswarapu et al., 2007; Shieh and Athanasiou, 2007), which applies controlled compressive loads onto single adherent cells. Cell to platen contact was determined by a 5 nN preload, followed by compression to 25 nN. At equilibrium deformation, chondrocytes were fixed with paraformaldehyde. After fixation, a phalloidin stain was applied for the cytoskeleton and a Hoescht's stain was applied for the nucleus. Both loaded and unloaded (control) cells were imaged with a confocal microscope, followed by three-dimensional image reconstructions. The use of fluorescent staining to examine cellular and nuclear deformations and strains has been previously described in the literature (Knight et al., 1998; Knight et al., 2002).

In an initial coarse search, cytoplasmic and nuclear Young's moduli were varied parametrically at 0.5 kPa increments from 1 to 7 kPa for combinations of Poisson's ratios shown in Table 1. These search parameters were guided by literature values for Poisson's ratios and cellular stiffness (Freeman et al., 1994; Leipzig and Athanasiou, 2005; Shieh and Athanasiou, 2006; Trickey et al., 2006; Leipzig and Athanasiou, 2008), as well as preliminary analyses confirming Young's moduli less than 1 kPa and Poisson's ratios less than 0.3 yielded higher δ_{RMS} values.

Based on results from the coarse search, Young's moduli were refined to increment 0.25 kPa from 3 to 5.5 kPa for $\nu_{Cyto} = \nu_{Nuc} = 0.5$ and $\nu_{Cyto} = 0.4$, $\nu_{Nuc} = 0.5$. Simulations were also performed for the cell without a nuclear inclusion to examine the contribution of the nucleus. For these cases, the cell was considered to be an isotropic linearly elastic solid with the same initial physical dimensions as before. For the cell model, cost function values were calculated using only cytoplasmic axial and lateral strains.

Due to the inherent variability in any cell mechanics technique and analysis, the finite element model was examined for its sensitivity to slight changes in the experimental data of Leipzig and Athanasiou (2008). The following three cases were studied: (1) increased axial and lateral cytoplasmic strains by 5%; (2) decreased axial and lateral nuclear strains by 5%; and (3) increased cytoplasmic strains by 5% and decreased nuclear strains by 5%. Finite element analysis was performed on the aforementioned cases for $\nu_{Cyto} = \nu_{Nuc} = 0.5$ to yield stiffness values for the cytoplasm and the nucleus.

3. Results

Table 1 shows minimum values computed from the cost function for each combination of Poisson's ratios, and the values of cytoplasmic and nuclear Young's moduli for which the minimum was obtained. From the initial coarse search, the ratio of cytoplasmic to nuclear stiffness was either ~1.4 ($E_Y^{Cyto} = 3.5$ kPa, $E_Y^{Nuc} = 5$ kPa) or ~1.1 ($E_Y^{Cyto} = 4$ kPa, $E_Y^{Nuc} = 4.5$ kPa) depending upon Poisson's ratios used. The minimum δ_{RMS}, or case most closely matching the experimental data, occurred for $\nu_{Cyto} = \nu_{Nuc} = 0.5$, i.e., both cytoplasm and nucleus incompressible. Fig. 1 shows the cell in its undeformed and deformed states for this minimum δ_{RMS} case. Comparing cases where cytoplasmic and nuclear Poisson's ratios were held equal, there was little effect of Poisson's ratio on δ_{RMS}, though the $\nu_{Cyto} = \nu_{Nuc} = 0.3$ case had a different "best fit" Young's moduli than the $\nu_{Cyto} = \nu_{Nuc} = 0.4$ or $\nu_{Cyto} = \nu_{Nuc} = 0.5$ cases.

Fig. 2 shows a 3-D plot of δ_{RMS} as a function of E_Y^{Cyto} and E_Y^{Nuc} for $\nu_{Cyto} = \nu_{Nuc} = 0.5$. In this refined search, the minimum Young's moduli were determined to be $E_Y^{Cyto} = 3.75$ kPa and $E_Y^{Nuc} = 5.25\,kPa$, with $\delta_{RMS} = 0.02276$. In the refined search for $\nu_{Cyto} = 0.4$ and $\nu_{Nuc} = 0.5$, minimum Young's moduli were determined to be $E_Y^{Cyto} = 4.0$ kPa and $E_Y^{Nuc} = 4.75$ kPa, with $\delta_{RMS} = 0.02572$. Without a nuclear inclusion, $E_Y^{Cell} = 4.25$ kPa, which did not change for $\nu_{Cell} = 0.4$ or 0.5.

Finally, experimental strains were varied to ascertain the effects of the experimental measurements on the ratio of cytoplasmic to nuclear stiffnesses. Slight changes in the experimental data of Leipzig and Athanasiou, (2008) did not yield substantial differences in the calculated stiffness for the cytoplasm and nucleus. In the case. where the experimentally measured axial and lateral cytoplasmic strains were increased by 5%, the Young's moduli were determined to be $E_Y^{Cyto} = 3.0$ kPa and $E_Y^{Nuc} = 5.5$ kPa. In the alternative case, where the experimentally measured axial and lateral nuclear strains were decreased by 5%, the Young's moduli were determined to be $E_Y^{Cyto} = 3.5$ kPa and $E_Y^{Nuc} = 6.0$ kPa. Finally, when the cytoplasmic strains were increased by 5% and nuclear strains decreased by 5%, the Young's moduli were determined to be $E_Y^{Cyto} = 3.0$ kPa and $E_Y^{Nuc} = 6.0$ kPa, yielding a nuclear to cytoplasmic stiffness ratio of 2.0.

4. Discussion

Using a finite element approach, this study investigated *in situ* mechanical properties of the nucleus. Young's moduli and Poisson's ratio were parametrically changed for the cytoplasm and nucleus, and predicted cellular and nuclear strains were compared to known experimental results during unconfined cytocompression (Leipzig and Athanasiou, 2008). It was found that the experimental data were best-matched when

$E_Y^{Cyto} = 3.75$ kPa, $E_Y^{Nuc} = 5.25$ kPa, and both cytoplasm and nucleus were incompressible. These results suggest that the ratio of nuclear to cytoplasmic stiffness is less than previously reported for single cells (Guilak, 2000; Caille et al., 2002). Moreover, changing Poisson's ratio had little effect on the model.

Examining nuclear mechanical properties is an important step toward understanding cellular mechanotransduction. Nuclear physical characteristics change in response to an applied load on native tissue (Guilak et al., 1995) or tissue-engineered constructs (Lee et al., 2000). Enclosed within the nucleus, chromatin is organized by the nuclear lamina (Aebi et al., 1986). Due to cellular deformations, mechanical linkages between cytoskeleton and nuclear lamina may lead to changes in chromatin conformation/alignment and/or 3-D spatial orientation of transcription factors. Thus, understanding how the nucleus senses and responds to forces provides insight into possible gene regulatory mechanisms.

The results presented in this study have applicability to current finite element models of cell–matrix interactions. These models predict the local mechanical environment of chondrocytes under various loading conditions (Guilak and Mow, 2000; Wu and Herzog, 2000; Breuls et al., 2002; Wang et al., 2002). When considering the cell without a nuclear inclusion, cellular Young's modulus was minimally greater than the cytoplasm itself. Moreover, the *in situ* difference between cytoplasmic and nuclear stiffnesses during compression is small, and variations in Poisson's ratio had little effect on Young's moduli (i.e., $E_Y^{Cyto} = 3.75$ kPa, $E_Y^{Nuc} = 5.25$ kPa for $\nu_{Cyto} = \nu_{Nuc} = 0.5$ versus $E_Y^{Cyto} = 4$ kPa, $E_Y^{Nuc} = 4.75$ kPa for $\nu_{Cyto} = 0.4$, $\nu_{Nuc} = 0.5$). These results suggest that assumptions of cellular homogeneity and incompressibility may be valid simplifications for theoretical models describing chondrocytes. Supporting these simplifications, no volume change has been measured experimentally in single chondrocytes subjected to unconfined compression at strain levels below ~30–35% (Koay et al., 2008).

Several explanations exist for why our results differ from previously reported nuclear and cellular stiffnesses. We observed a nuclear to cytoplasmic stiffness ratio of ~1.1 or ~1.4 depending

Table 1
Effect of Poisson's ratio combinations on cytoplasmic and nuclear stiffnesses for the initial coarse search.

Poisson's ratio		"Best fit" stiffness		
Cytoplasm	Nucleus	Cytoplasm (kPa)	Nucleus (kPa)	δ_{RMS}
0.3	0.3	4	4.5	0.03770
0.3	0.4	4	4.5	0.03360
0.4	0.3	3.5	5	0.03357
0.4	0.4	3.5	5	0.03018
0.4	0.5	4	4.5	0.02595
0.5	0.4	3.5	5	0.02627
0.5	0.5	3.5	5	0.02279

In the coarse search, cytoplasmic and nuclear stiffness values were each varied parametrically from 1 to 7 kPa, resulting in 169 different stiffness combinations for each set of Poisson's ratio values. In the coarse search, it was observed that the $\nu_{Cyto} = \nu_{Nuc} = 0.5$ combination best fit the experimental data with the lowest cost function value, resulting in $E_Y^{Cyto} = 3.5\,kPa$, $E_Y^{Nuc} = 5\,kPa$. The similarity of "best fit" stiffnesses and cost function demonstrate that Poisson's ratio had little effect on the ratio of cytoplasmic to nuclear stiffness.

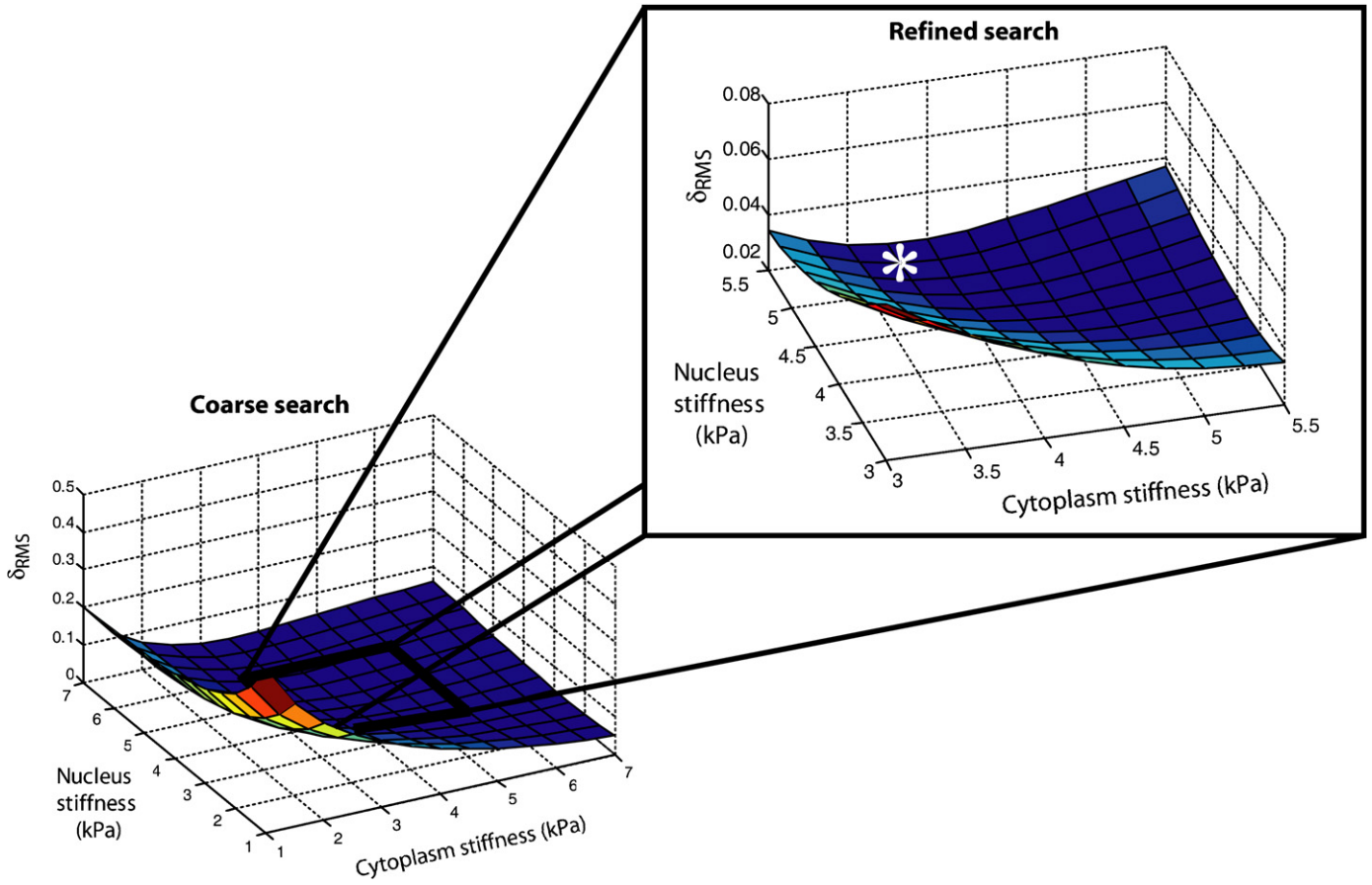

Fig. 2. Cost function (δ_{RMS}) plots for the case of $\nu_{Cyto} = \nu_{Nuc} = 0.5$. In the initial coarse search, the elastic moduli of the cytoplasm and nucleus were varied from 1 to 7 kPa, at 0.5 kPa increments. In the exploded view, the search was refined to range from 3 to 5.5 kPa, at 0.25 kPa increments. A global minimum for δ_{RMS} was observed at $E_Y^{Cyto} = 3.75$ kPa, $E_Y^{Nuc} = 5.25$ kPa (indicated by the asterisk).

on the assumed combination of Poisson's ratios, whereas prior results from micropipette aspiration testing of chondrocytes and isolated nuclei suggest this ratio is 3–4 (Guilak et al., 2000). However, in comparison to the free-floating state in micropipette aspiration, cytoskeletal rearrangements during cell attachment for unconfined cytocompression may cause alterations in nuclear structure and decreased stiffness. Moreover, when tested *in situ*, connections between the nuclear lamina and cytoskeleton are intact, resulting in a more integrated mechanical framework between the cytoplasm and nucleus. Further, the cellular stiffness under compression is greater than previous micropipette aspiration results with single chondrocytes (Trickey et al., 2000), in which tensile forces dominate. Prior literature has confirmed that cell stiffness is greater during bulk cell compression than during local aspiration of the cell membrane (Trickey et al., 2000; Bader et al., 2002; Shieh and Athanasiou, 2006).

It is further important to note that the stiffness values for single chondrocytes calculated in this study coincide with measurements obtained by Knight and Bader (Knight et al., 2002) for cells compressed within alginate constructs. In both unconfined cytocompression and cell compression within constructs, single cells must withstand compressive forces applied onto the whole cell, and thus a similar mechanical response is expected. Additionally, the predicted stiffness value of the overall cell using our model is 2–3 times greater than previous unconfined compression results for single chondrocytes (Leipzig and Athanasiou, 2005; Shieh and Athanasiou, 2006). Since our finite element model represents the cell as an ellipsoid, which more accurately resembles the geometry of attached chondrocytes than a cylinder (Shieh et al., 2006), the increased stiffness is likely an effect of modeling the changing contact surface area. The contact area between the cell (represented by our geometry) and the platen in the compressed state at equilibrium is 28% of that obtained assuming the entire cell's cross-section is in contact under compression (cylindrical geometry). Thus, for the same applied force, the stress experienced by our cell would be approximately 3.6 times greater than that of a cell with an assumed cylindrical geometry. Smaller contact area results in increased stress and, hence, greater cell stiffness.

Several assumptions were made for this model which could limit its representation of physical reality. First, the assumption of a spherical nucleus can potentially affect the resultant properties of the cytoplasm and nucleus. Changes in nucleus size, morphology, uniformity, and connections with the cytoplasm may alter the stress distributions applied on the nucleus, thereby changing the calculated stiffness of the nucleus. For instance, a larger contact area between the nucleus and cytoplasm could decrease the stress in the nucleus, resulting in a lower nuclear stiffness. In addition, preferential interactions between the nucleus and cytoskeleton could result in non-uniform nuclear deformations, changing the calculated stiffness values. In this study, we choose to assume a simple spherical geometry because previous finite element modeling (Vaziri and Mofrad, 2007) and experimental data (Guilak, 1995) have used or suggested, respectively, a spherical nucleus. An additional limitation is that the cell is assumed to be in frictionless contact with the platen, which is inherently difficult to verify experimentally. This may result in variations in cell stiffness and, thus, different cytoplasmic to nuclear stiffness ratios. However, as mentioned in the previous paragraph, the high cell stiffness reported in this study may also be due to a more accurate representation of cellular geometry (Koay et al., 2008). Finally, this model assumed both the cytoplasm and nucleus to be isotropic materials. Differences in the Poisson's ratio between principal directions can alter the axial and lateral strains and, thus, the calculated material properties. However, the experimental results presented by Leipzig and Athanasiou (2008) suggest a deviation from isotropy only at loads 50 nN or greater. At the 25 nN load case examined in this study, the experimental Poisson's ratio values for the cell and nucleus were 0.45 and 0.42, respectively. These values have been confirmed with other experimental testing modalities, generally yielding Poisson's ratios between 0.3 and 0.5 (Freeman et al., 1994; Shieh and Athanasiou, 2006; Trickey et al., 2006). Thus, based on previous experimental work at the low loads and strains examined in our model, anisotropy was not considered. In the future, this model can be adapted to include consideration of varying nuclear morphologies, cytoskeletal and nuclear interactions, frictional contact between the cell and the compressing platen, and anisotropies.

In conclusion, this study elucidated a combination of chondrocyte cytoplasmic and nuclear stiffnesses and Poisson's ratios which simulated previous results for unconfined cytocompression. *In situ*, nuclear stiffness was determined to be 40% more than the cytoplasm, which is lower than previously reported (Guilak et al., 2000; Caille et al., 2002). Moreover, little effect of Poisson's ratio on the model's behavior was observed, and the incompressible case best-matched the prior experimental data. These results have implications in understanding the basis of cellular mechanotransduction.

Conflict of interest statement

None

Acknowledgements

The authors gratefully acknowledge Dr. Nic Liepzig for generating the experimental data to which the modeling results were compared, Dr. Michael Liebschner for allowing access to the computer on which the simulations were run, and Ms. Eileen Meyer for helping automate ABAQUS simulations. Funding support for Mr. Ofek was provided by a training fellowship from the Nanobiology Training Program of the W. M. Keck Center for Interdisciplinary Bioscience Training of the Gulf Coast Consortia (NIH Grant nos. 5 T90 DK70121-03 and 5 R90 DK71504-03).

References

Aebi, U., Cohn, J., Buhle, L., Gerace, L., 1986. The nuclear lamina is a meshwork of intermediate-type filaments. Nature 323, 560–564.
Bader, D.L., Ohashi, T., Knight, M.M., Lee, D.A., Sato, M., 2002. Deformation properties of articular chondrocytes: a critique of three separate techniques. Biorheology 39, 69–78.
Breuls, R.G., Sengers, B.G., Oomens, C.W., Bouten, C.V., Baaijens, F.P., 2002. Predicting local cell deformations in engineered tissue constructs: a multilevel finite element approach. J. Biomech. Eng. 124, 198–207.
Buschmann, M.D., Hunziker, E.B., Kim, Y.J., Grodzinsky, A.J., 1996. Altered aggrecan synthesis correlates with cell and nucleus structure in statically compressed cartilage. J. Cell Sci. 109 (Pt 2), 499–508.
Caille, N., Thoumine, O., Tardy, Y., Meister, J.J., 2002. Contribution of the nucleus to the mechanical properties of endothelial cells. J. Biomech. 35, 177–187.
Eleswarapu, S.V., Leipzig, N.D., Athanasiou, K.A., 2007. Gene expression of single articular chondrocytes. Cell Tissue Res. 327, 43–54.
Freeman, P.M., Natarajan, R.N., Kimura, J.H., Andriacchi, T.P., 1994. Chondrocyte cells respond mechanically to compressive loads. J. Orthop. Res. 12, 311–320.
Guilak, F., 1995. Compression-induced changes in the shape and volume of the chondrocyte nucleus. J. Biomech. 28, 1529–1541.
Guilak, F., 2000. The deformation behavior and viscoelastic properties of chondrocytes in articular cartilage. Biorheology 37, 27–44.
Guilak, F., Mow, V.C., 2000. The mechanical environment of the chondrocyte: a biphasic finite element model of cell-matrix interactions in articular cartilage. J. Biomech. 33, 1663–1673.
Guilak, F., Ratcliffe, A., Mow, V.C., 1995. Chondrocyte deformation and local tissue strain in articular cartilage: a confocal microscopy study. J. Orthop. Res. 13, 410–421.
Guilak, F., Tedrow, J.R., Burgkart, R., 2000. Viscoelastic properties of the cell nucleus. Biochem. Biophys. Res. Commun. 269, 781–786.

Knight, M.M., Ghori, S.A., Lee, D.A., Bader, D.L., 1998. Measurement of the deformation of isolated chondrocytes in agarose subjected to cyclic compression. Med. Eng. Phys. 20, 684–688.

Knight, M.M., van de Breevaart Bravenboer, J., Lee, D.A., van Osch, G.J., Weinans, H., Bader, D.L., 2002. Cell and nucleus deformation in compressed chondrocyte-alginate constructs: temporal changes and calculation of cell modulus. Biochim. Biophys. Acta 1570, 1–8.

Koay, E.J., Ofek, G., Athanasiou, K.A., 2008. Effects of TGF-beta1 and IGF-I on the compressibility, biomechanics, and strain-dependent recovery behavior of single chondrocytes. J. Biomech. 41, 1044–1052.

Lee, D.A., Knight, M.M., Bolton, J.F., Idowu, B.D., Kayser, M.V., Bader, D.L., 2000. Chondrocyte deformation within compressed agarose constructs at the cellular and sub-cellular levels. J. Biomech. 33, 81–95.

Leipzig, N.D., Athanasiou, K.A., 2005. Unconfined creep compression of chondrocytes. J. Biomech. 38, 77–85.

Leipzig, N.D., Athanasiou, K.A., 2008. Static compression of single chondrocytes catabolically modifies single-cell gene expression. Biophys. J. 94, 2412–2422.

Leipzig, N.D., Eleswarapu, S.V., Athanasiou, K.A., 2006. The effects of TGF-beta1 and IGF-I on the biomechanics and cytoskeleton of single chondrocytes. Osteoarthritis Cartilage.

Maniotis, A.J., Chen, C.S., Ingber, D.E., 1997. Demonstration of mechanical connections between integrins, cytoskeletal filaments, and nucleoplasm that stabilize nuclear structure. Proc. Natl. Acad. Sci. U S A 94, 849–854.

Shieh, A.C., Athanasiou, K.A., 2006. Biomechanics of single zonal chondrocytes. J. Biomech. 39, 1595–1602.

Shieh, A.C., Athanasiou, K.A., 2007. Dynamic compression of single cells. Osteoarthritis Cartilage 15, 328–334.

Shieh, A.C., Koay, E.J., Athanasiou, K.A., 2006. Strain-dependent recovery behavior of single chondrocytes. Biomech. Model Mechanobiol. 5, 172–179.

Trickey, W.R., Baaijens, F.P., Laursen, T.A., Alexopoulos, L.G., Guilak, F., 2006. Determination of the Poisson's ratio of the cell: recovery properties of chondrocytes after release from complete micropipette aspiration. J. Biomech. 39, 78–87.

Trickey, W.R., Lee, G.M., Guilak, F., 2000. Viscoelastic properties of chondrocytes from normal and osteoarthritic human cartilage. J. Orthop. Res. 18, 891–898.

Vaziri, A., Mofrad, M.R., 2007. Mechanics and deformation of the nucleus in micropipette aspiration experiment. J. Biomech. 40, 2053–2062.

Wang, C.C., Guo, X.E., Sun, D., Mow, V.C., Ateshian, G.A., Hung, C.T., 2002. The functional environment of chondrocytes within cartilage subjected to compressive loading: a theoretical and experimental approach. Biorheology 39, 11–25.

Wang, N., Butler, J.P., Ingber, D.E., 1993. Mechanotransduction across the cell surface and through the cytoskeleton. Science 260, 1124–1127.

Wu, J.Z., Herzog, W., 2000. Finite element simulation of location- and time-dependent mechanical behavior of chondrocytes in unconfined compression tests. Ann. Biomed. Eng. 28, 318–330.